J|A|C|S ARTICLES

Published on Web 08/10/2010

Quantitative Catalyst−Substrate Association Relationships between Metathesis Molybdenum or Ruthenium Carbene Complexes and Their Substrates

Kyung Hwan Kim,[†] Taedong Ok,[‡,§] Kwangyeol Lee,[||] Hee-Seung Lee,[§] Kyu Tae Chang,[⊥] Hyotcherl Ihee,*[,†] and Jeong-Hun Sohn*[,‡]

Center for Time-Resolved Diffraction, Department of Chemistry, Graduate School of Nanoscience & Technology (WCU), KAIST, Daejeon, Korea, Institut Pasteur Korea, Seongnam, Korea, Molecular-Level Interface Research Center, Department of Chemistry, KAIST, Daejeon, Korea, Department of Chemistry, Korea University, Seoul, Korea, and The National Primate Research Center, Korea Research Institute of Bioscience and Biotechnology, Ochang, Korea

Received May 15, 2010; E-mail: sohnjh@ip-korea.org; hyotcherl.ihee@kaist.ac.kr

Abstract: Herein we present the long-sought quantitative catalyst−substrate association relationships based on experimentally measured quantitative association preferences of diverse metathesis Mo and Ru catalysts (**Mo-1**, Schrock Mo; **Mo-2**, Schrock−Hoveyda Mo; **Ru-1**, Grubbs first generation Ru; **Ru-2**, Grubbs second generation Ru; **Ru-3**:, Grubbs−Hoveyda first generation Ru; and **Ru-4**, Grubbs−Hoveyda second generation Ru) to their substrates (alkenes, alkynes and allenes), determined directly by a general method based on FRET principle. The determined substrate preferences are proved to be dependent on the molecular identity of the catalyst, exhibiting the preference order of alkyne > alkene > allene for **Mo-1** and **Mo-2**, allene > alkene > alkyne for **Ru-1** and **Ru-3**, and alkyne > allene > alkene for **Ru-2** and **Ru-4**. The results enable us to probe metathesis mechanisms by answering issues in metathesis reactions including the controversial reaction initiation in enyne or allenyne metathesis.

Introduction

The discovery of Mo and Ru carbene complexes by Schrock and Grubbs in 1990[1] and 1992,[2] respectively, has made rapid progress in synthetic organic chemistry.[3] The Mo and Ru carbenes are transition metal catalysts which can perform a variety of metathesis reactions among alkene, alkyne and allene substrates. The diversity of Mo- and Ru-based metathesis reactivity is reflected by the presence of numerous metathesis reactions including olefin metathesis,[4] enyne metathesis,[5] allene metathesis,[6] diyne metathesis,[7] and allenyne metathesis.[8]

Great advances have been made in terms of synthetic applications of the metathesis reactions, but there are still ambiguities in the mechanistic understanding, with the most salient unresolved fundamental issue being the catalyst−substrate association relationships. Although the association preference of a catalyst to a substrate among multiple candidate substrates dictates the identity of the initial adduct/intermediate that can determine the reaction pathway and the ultimate key propagating species with regioselectivity,[9] even the substrate-association preference of this famous class of catalyst and its dependence on the molecular identity of the catalyst have not been quantitatively determined. In particular, the reaction initiation in ring closing enyne metathesis has been a long-standing controversy,[10] much of which stems from the identical product from two equally plausible reaction pathways and the deduction

[†] Graduate School of Nanoscience & Technology (WCU), KAIST.
[‡] Institut Pasteur Korea.
[§] Department of Chemistry, KAIST.
[||] Korea University.
[⊥] Korea Research Institute of Bioscience and Biotechnology.

(1) Schrock, R. R.; Murdzek, J. S.; Bazan, G. C.; Robbins, J.; DiMare, M.; O'Regan, M. *J. Am. Chem. Soc.* **1990**, *112*, 3875.
(2) Nguyen, S.-B. T.; Johnson, L. K.; Grubbs, R. H. *J. Am. Chem. Soc.* **1992**, *114*, 3974.
(3) (a) Grubbs, R. H. *Adv. Synth. Catal.* **2007**, *349*, 34 (Nobel Lecture 2005). (b) Schrock, R. R. *Adv. Synth. Catal.* **2007**, *349*, 41 (Nobel Lecture 2005).
(4) For recent representative reviews on Ru catalyzed olefin metathesis, see: (a) Grubbs, R. H. *Tetrahedron* **2004**, *60*, 7117. (b) Schrock, R. R.; Czekelius, C. *Adv. Synth. Catal.* **2007**, *349*, 55. (c) Hoveyda, A. H.; Zhugralin, A. R. *Nature* **2007**, *450*, 243. For a special issue dedicated to olefin metathesis, see: (d) *Adv. Synth. Catal.* **2007**, *349*, issues 1−2.
(5) For recent representative reviews on the enyne metathesis, see: (a) Mori, M. *Materials* **2010**, *3*, 2087. (b) Diver, S. T.; Giessert, A. J. *Chem. Rev.* **2004**, *104*, 1317. (c) Villar, H.; Frings, M.; Bolm, C. *Chem. Soc. Rev.* **2007**, *36*, 55. (d) Hansen, E. C.; Lee, D. *Acc. Chem. Res.* **2006**, *39*, 509. (e) Kotha, S.; Meshram, M.; Tiwari, A. *Chem. Soc. Rev.* **2009**, *38*, 2065. (f) Chattopadhyay, S. K.; Karmakar, S.; Biswas, T.; Majumdar, K. C.; Rahaman, H.; Roy, B. *Tetrahedron* **2007**, *63*, 3919. (g) Mulzer, J.; Oehler, E. *Top. Organomet. Chem.* **2004**, *13*, 269.
(6) (a) Ahmed, M.; Arnauld, T.; Barrett, A. G. M.; Braddock, D. C.; Flack, K.; Procopiou, P. A. *Org. Lett.* **2000**, *2*, 551. (b) Janssen, C. E.; Krause, N. *Eur. J. Org. Chem.* **2005**, *2005*, 2322.
(7) (a) Fox, H. H.; Wolf, M. O.; O'Dell, R.; Lin, B. L.; Schrock, R. R.; Wrighton, M. S. *J. Am. Chem. Soc.* **1994**, *116*, 2827. (b) Schrock, R. R.; Luo, S.; Lee, J. C. J.; Zanetti, N. C.; Davis, W. M. *J. Am. Chem. Soc.* **1996**, *118*, 3883.
(8) Murakami, M.; Kadowaki, S.; Matsuda, T. *Org. Lett.* **2005**, *7*, 3953.
(9) For representative reviews, see: (a) Gorin, D. J.; Toste, F. D. *Nature* **2007**, *446*, 395. (b) Saito, S.; Yamamoto, Y. *Chem. Rev.* **2000**, *100*, 2901. (c) Ojima, I.; Tzamarioudaki, M.; Li, Z.; Donovan, R. J. *Chem. Rev.* **1996**, *96*, 635.

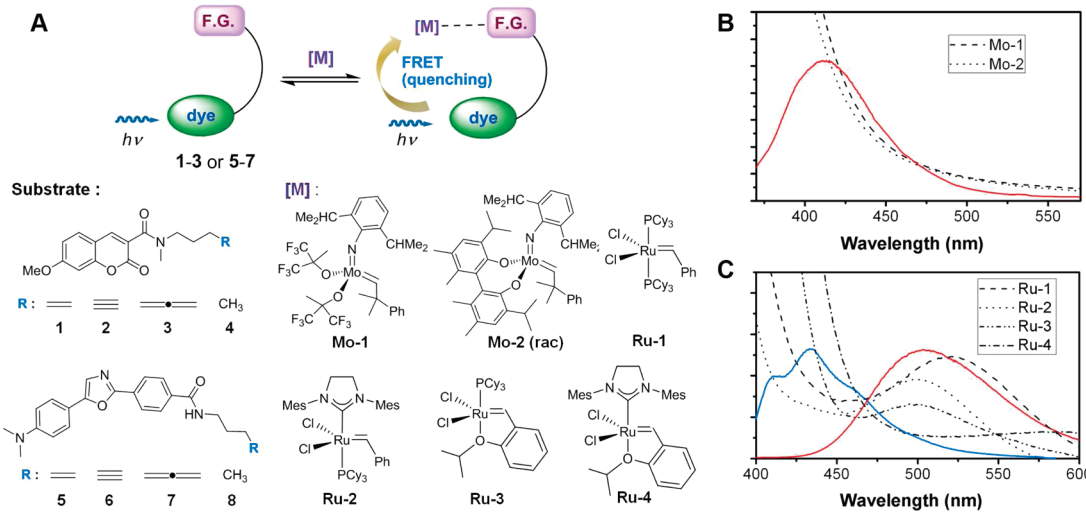

Figure 1. Quantitative substrate-association preferences of Mo and Ru catalysts for metathesis reaction. (A) Schematic illustration of probing the substrate-association preference of metathesis Mo and Ru carbene complexes. Mo carbenes (**Mo-1** and **Mo-2**) or Ru carbenes (**Ru-1**, **Ru-2**, **Ru-3** and **Ru-4**) act as quenchers of the coumarin or dapoxyl fluorophore, respectively, when dye-conjugated substrate is bound to the catalyst. (B) Black dashed/dotted lines are the UV−vis spectra of **Mo-1** and **Mo-2** (20 μM), and red line is the fluorescence spectrum of the dye molecule in toluene. (C) Black dashed/dotted lines are the UV−vis spectra of four Ru catalysts (20 μM) and colored solid lines are the fluorescence spectra of the dye molecule in CH_2Cl_2 (red) and *n*-hexane (blue).

of the very early event without direct observation. Theoretical interpretation of the results has been attempted previously,[11] but definitive experimental evidence is currently missing.

Due to the dearth of knowledge on the quantitative substrate preference, it could not be established how much the molecular identity of diverse metathesis Mo and Ru catalysts influences their substrate preferences and thus whether each Mo or Ru catalyst directs different reaction pathways in the presence of multiple substrates. Herein we report the quantitative catalyst−substrate association relationships of an exhaustive list of metathesis Mo and Ru catalysts to various substrates, and discuss their usefulness in answering previously unexplained observations in metathesis reactions and resolving the assumption on the controversial reaction initiation in enyne or allenyne metathesis.

Results and Discussion

Our plan for determining the substrate preferences of the Mo and Ru catalysts entailed bringing fluorescence resonance energy transfer (FRET) principle into effect (Figure 1).[12] Using the FRET-based method we directly detected the interactions between the catalysts (**Mo-1**, Schrock Mo; **Mo-2**, Schrock−Hoveyda Mo; **Ru-1**, Grubbs first generation Ru; **Ru-2**, Grubbs second generation Ru; **Ru-3**, Grubbs−Hoveyda first generation Ru; and **Ru-4**, Grubbs−Hoveyda second generation Ru) and dye-conjugated substrates (alkenes, alkynes and allenes). We determined both kinetic and thermodynamic parameters for the association event between the Mo or the Ru complexes and the substrates that provide direct and critical information on the substrate-association preferences of the catalysts and initial adduct/intermediate formation in the metathesis reactions.

Since all of the two Mo and four Ru catalysts have absorbance bands at visible range with no emission of fluorescence and thus could act as fluorescence quenchers, we chose two dyes, coumarin and dapoxyl dyes that have fluorescence emission bands near the absorbance bands of the Mo and Ru catalysts, respectively (Figure 1A). We prepared the substrates **1**−**8**, the coumarin- and the dapoxyl-conjugated terminal alkenes, alkynes, allenes and alkanes (controls) by attaching the desired functional groups to the dyes via an amide linkage with a three-carbon tether, as shown in Figure 1A. The emission bands of substrates **1**−**3** in toluene were observed at 412 nm, and those of substrates **5**−**7** were observed at 508 nm in CH_2Cl_2 and 432 nm in *n*-hexane, respectively (Figure 1B and 1C).

The time-dependent fluorescence quenching of substrates caused by each catalyst under various reaction conditions allowed for the simultaneous determination of k, k_{-1}, K_d and ΔG of each specific association event occurring in a given substrate/catalyst pair. Some examples of the time-dependent fluorescence spectra of the substrates are shown in Figure 2 for the six catalysts, and the time-dependent fluorescence traces (integrated values of fluorescence spectra) for all possible combinations of the six catalysts and the six substrates are plotted in Figure 3. During the fluorescence quenching, no significant absorbance change of the substrate due to the energy transfer between the substrates was observed (see Supporting Information), confirming that it is the catalyst that is responsible for the fluorescence quenching.

The dependence of the fluorescence quenching rate on the substrate is clearly seen for each catalyst. For example, Figure 3A exhibits substrate-dependent, disparate fluorescence quenching rates of the three coumarin-conjugated substrates for catalyst **Mo-1** with λ_{max} = 364 nm, which is fastest for alkyne **2** with the decreasing rate order of alkyne **2** > alkene **1** > allene **3**. For each catalyst, the fluorescence quenching traces for the three substrates under various reaction conditions were simultaneously

(10) (a) Kim, S. H.; Bowden, N.; Grubbs, R. H. *J. Am. Chem. Soc.* **1994**, *116*, 10801. (b) Hoye, T. R.; Donaldson, S. M.; Vos, T. J. *Org. Lett.* **1999**, *1*, 277. (c) Schramm, M. P.; Reddy, D. S.; Kozmin, S. A. *Angew. Chem., Int. Ed.* **2001**, *40*, 4274. (d) Hansen, E. C.; Lee, D. *J. Am. Chem. Soc.* **2003**, *125*, 9582. (e) Lee, H.-Y.; Kim, B. G.; Snapper, M. L. *Org. Lett.* **2003**, *5*, 1855. (f) Lloyd-Jones, G. C.; Margue, R. G.; de Vries, J. G. *Angew. Chem., Int. Ed.* **2005**, *44*, 7442. (g) Diver, S. T.; Galan, B. R.; Giessert, A. J.; Keister, J. B. *J. Am. Chem. Soc.* **2005**, *127*, 5762. (h) Lee, Y.-J.; Schrock, R. R.; Hoveyda, A. H. *J. Am. Chem. Soc.* **2009**, *131*, 10652.
(11) Lippstreu, J. J.; Straub, B. F. *J. Am. Chem. Soc.* **2005**, *127*, 7444.
(12) Sohn, J.-H.; Kim, K. H.; Lee, H.-Y.; No, Z. S.; Ihee, H. *J. Am. Chem. Soc.* **2008**, *130*, 16506.

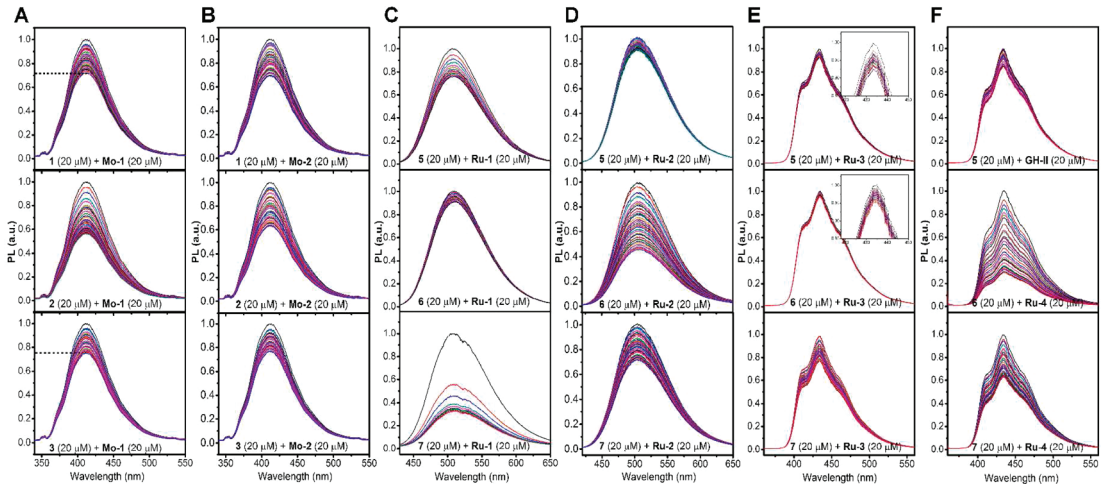

Figure 2. Time-dependent change of the fluorescence spectra of dye−alkene (**1** or **5**), dye−alkyne (**2** or **6**) and dye−allene (**3** or **7**) due to the reaction with the (A) **Mo-1**, (B) **Mo-2**, (C) **Ru-1**, (D) **Ru-2**, (E) **Ru-3** and (F) **Ru-4** catalysts. For each pair of a catalyst and a substrate, multiple experimental conditions (for example, 20 μM:20 μM and 10 μM:20 μM of substrate vs catalyst and mixed substrates for some cases) were used to increase the information content of data, and here the time-dependent spectra for only one condition (20 μM:20 μM) are shown.

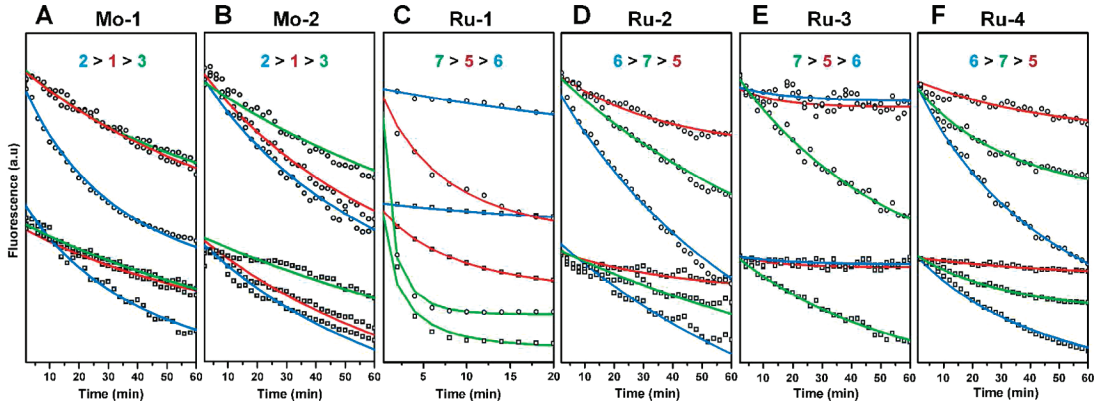

Figure 3. Time-dependent fluorescence quenching of the dye-conjugated substrates (alkenes **1** and **5**, alkynes **2** and **6**, and allenes **3** and **7**) by six types of catalysts, (A) **Mo-1**, (B) **Mo-2**, (C) **Ru-1**, (D) **Ru-2**, (E) **Ru-3**, and (F) **Ru-4**. Experimental data points are shown as black circles and squares (20 μM:20 μM and 10 μM:20 μM of substrate vs catalyst, respectively), and the theoretical curves from the global fitting analysis are represented as red, blue and green solid lines for alkenes **1** and **5**, alkynes **2** and **6**, and allenes **3** and **7**, respectively. The black circles (20 μM:20 μM) correspond to the integrated values of the fluorescence spectra shown in Figure 2. Fitting was done by using a simple kinetic model (see Supporting Information), and it elucidates the kinetic and thermodynamic behavior of the association of the catalyst with the substrate. The orderings of substrate-association preference of each catalyst are shown at the top of the each panel.

fitted against a set of rate equations (see Supporting Information), and the results are shown in Table 1. The obtained rate coefficients and the Gibbs free energy for the association process between the substrate and the catalyst provide more quantitative information for the substrate preference of each catalyst than can be visualized from Figure 3.

Generally the final product can be reached via various reaction pathways and each reaction pathway may consist of multiple reaction steps. The rate determining step is the one with the highest reaction barrier along a reaction pathway and depends on the identity of the catalyst used in the reaction. According to previous studies, for Mo-catalyzed olefin metathesis reaction, it has been shown that the initial substrate association step is the rate determining step.[13] Thus, our experimentally obtained substrate preferences can be safely used to rationalize the suggested mechanisms in Mo-catalyzed metathesis reactions.

For catalyst **Mo-1**, the substrate preference order of alkyne > alkene > allene, shown in Figure 3 and Table 1, is in line with the common assumption that ring closing enyne metathesis catalyzed by group VI (Cr, Mo, W) complexes initiates at alkyne (path B in Figure 4A),[14] and the exclusive *endo*-product formations in the reactions using Mo complexes through metallacyclobutene intermediates.[10h] The stronger preference of **Mo-1** to alkyne than allene can also resolve the mechanism of the ring closing allenyne metathesis using **Mo-1**, along with the observation of byproduct **A** and the complete consumption of alkyne with remaining allene intact in the attempted intermolecular allenyne metathesis using **Mo-1** (Figure 4B),[8] indicating the reaction initiation at alkyne.[4b]

The Schrock−Hoveyda catalyst (**Mo-2**) with $\lambda_{max} = 361$ nm possesses the same order of substrate preference as the Schrock catalyst (**Mo-1**) both kinetically and thermodynamically, which is alkyne **2** > alkene **1** > allene **3** (Figure 3B and Table 1). Considering their similar electronic and molecular structures,

(13) Poater, A.; Solans-Monfort, X.; Clot, E.; Coperet, C.; Eisenstein, O. *J. Am. Chem. Soc.* **2007**, *129*, 8207.

(14) (a) Katz, T. J.; Sivavec, T. M. *J. Am. Chem. Soc.* **1985**, *107*, 737. (b) Korkowski, P. F.; Hoye, T. R.; Rydberg, D. B. *J. Am. Chem. Soc.* **1988**, *110*, 2676. (c) Watanuki, S.; Ochifuji, N.; Mori, M. *Organometallics* **1994**, *13*, 4129.

Table 1. Kinetic and Thermodynamic Parameters for Alkenes **1** and **5**, Alkynes **2** and **6**, and Allenes **3** and **7** with Each Mo and Ru Catalyst Determined by the Data Analysis[a]

catalyst	substrate	k (M^{-1} s^{-1})	rel k[b]	k_{-1} (s^{-1})	K_d (k_{-1}/k)	ΔG (kJ/mol)	rel stability[c]
Mo-1	**1**	$6.54(\pm2.51) \times 10^2$	1	$3.45(\pm1.45) \times 10^{-3}$	$5.28(\pm3.00) \times 10^{-6}$	-29.6 ± 1.38	1
	2	$1.81(\pm0.67) \times 10^3$	2.77	$2.50(\pm0.88) \times 10^{-3}$	$1.39(\pm0.70) \times 10^{-6}$	-32.9 ± 1.23	3.80
	3	$6.07(\pm0.87) \times 10^2$	0.93	$3.56(\pm1.41) \times 10^{-3}$	$5.87(\pm2.50) \times 10^{-6}$	-29.3 ± 1.03	0.90
Mo-2	**1**	$8.75(\pm3.07) \times 10^2$	1	$1.28(\pm1.95) \times 10^{-5}$	$1.46(\pm2.29) \times 10^{-8}$	-43.9 ± 3.78	1
	2	$1.05(\pm0.34) \times 10^3$	1.2	$1.52(\pm2.71) \times 10^{-6}$	$1.46(\pm2.63) \times 10^{-9}$	-49.6 ± 4.44	10.0
	3	$4.67(\pm2.15) \times 10^2$	0.53	$2.57(\pm3.53) \times 10^{-5}$	$5.51(\pm7.95) \times 10^{-8}$	-40.7 ± 3.53	0.26
Ru-1	**5**	$3.71(\pm0.13) \times 10^3$ [d]	1	$2.12(\pm0.23) \times 10^{-2}$ [d]	$5.71(\pm0.65) \times 10^{-6}$	-29.4 ± 0.03[d]	1
	6	$2.60(\pm0.09) \times 10^2$ [d]	0.07	$9.81(\pm8.15) \times 10^{-3}$ [d]	$3.77(\pm3.14) \times 10^{-5}$	-24.8 ± 2.03[d]	0.15
	7	$5.25(\pm0.53) \times 10^4$	14.2	$8.71(\pm1.59) \times 10^{-3}$	$1.66(\pm0.35) \times 10^{-7}$	-38.0 ± 0.05	34.4
Ru-2	**5**	$1.19(\pm0.33) \times 10^2$	1	$1.98(\pm1.39) \times 10^{-2}$	$1.66(\pm1.26) \times 10^{-4}$	-21.9 ± 1.90	1
	6	$2.98(\pm0.34) \times 10^2$	2.50	$5.26(\pm4.05) \times 10^{-4}$	$1.77(\pm1.37) \times 10^{-6}$	-33.4 ± 1.96	93.8
	7	$1.63(\pm0.27) \times 10^2$	1.37	$2.79(\pm0.33) \times 10^{-3}$	$1.71(\pm0.35) \times 10^{-5}$	-27.6 ± 0.51	9.70
Ru-3	**5**	$4.34(\pm5.29) \times 10^1$	1	$6.96(\pm9.31) \times 10^{-2}$	$1.60(\pm2.90) \times 10^{-3}$	-16.2 ± 4.56	1
	6	$2.55(\pm2.62) \times 10^1$	0.59	$5.64(\pm8.72) \times 10^{-2}$	$2.21(\pm4.11) \times 10^{-3}$	-15.4 ± 4.68	0.72
	7	$1.19(\pm0.29) \times 10^2$	2.60	$1.25(\pm0.91) \times 10^{-2}$	$1.05(\pm0.80) \times 10^{-4}$	-23.1 ± 1.93	15.2
Ru-4	**5**	$1.10(\pm0.53) \times 10^2$	1	$1.62(\pm1.78) \times 10^{-2}$	$1.47(\pm1.77) \times 10^{-4}$	-22.2 ± 3.02	1
	6	$8.63(\pm0.42) \times 10^2$	7.85	$1.31(\pm4.67) \times 10^{-5}$	$1.52(\pm5.41) \times 10^{-8}$	-45.4 ± 8.98	9670
	7	$4.98(\pm0.87) \times 10^2$	4.53	$1.45(\pm0.63) \times 10^{-2}$	$2.91(\pm1.36) \times 10^{-5}$	-26.3 ± 1.18	5.05

[a] k and k_{-1} are directly determined as fitting parameters, and K_d and ΔG are calculated with proper equations, k_{-1}/k and $-RT \ln(1/K_d)$, repectively. k and ΔG represent the kinetic and theromodynamic preferences respectively. [b] Relative speed of the association reaction. The k of alkene (**1** or **5**) is defined as 1. [c] Relative thermodynamic stability of the associated complex. The K_d of alkene−catalyst complex is defined as 1. [d] Values referred from our previous study.[12]

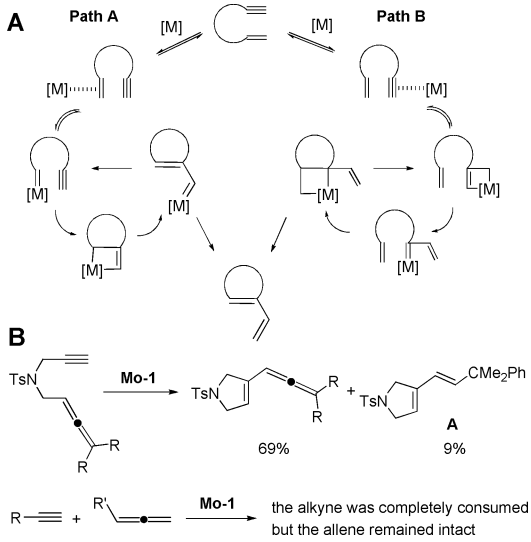

Figure 4. Some examples of metathesis reaction patterns using Mo carbene that have been previously unexplained but can be explained in light of the determined substrate-association preference ordering. (A) The substrate preference order of alkyne > alkene > allene is in line with the common assumption that ring closing enyne metathesis catalyzed by group VI complexes initiates at alkyne (path B).[14] (B) Ring-closing allenyne metathesis catalyzed by **Mo-1**. Along with the observation of byproduct **A** and the complete consumption of alkyne with remaining allene intact in the attempted intermolecular allenyne metathesis using **Mo-1**,[8] the stronger preference of **Mo-1** to alkyne than to allene can resolve the mechanism, indicating the reaction initiation at alkyne.[4b]

the same preference order is anticipated although some differences are observed for the relative fluorescence quenching rates between the substrates, which might be due to the different electronic effect between alkoxides and phenoxides of the catalysts. This is the first time that the exact ordering of the substrate preference has been quantitatively determined for both **Mo-1** and **Mo-2** with all their metathesis substrates, alkene, alkyne and allene.

Unlike Schrock and Schrock−Hoveyda catalysts, the Grubbs first generation catalyst (**Ru-1**) with $\lambda_{max} = 527$ nm possesses completely reverse substrate preference, allene **7** > alkene **5**[12] > alkyne **6**,[12] both kinetically and thermodynamically (Figure 3C and Table 1). Although allene metathesis reaction has not drawn much attention from synthetic chemists and, to our best knowledge, only two bisallene metathesis[6] and one allenyne metathesis[8] have been reported, our results may stimulate intense research on the metathesis reactions with allene substrate as well as allene transformation reactions catalyzed by other transition metal catalysts.

Different from the case of **Ru-1**, the time-dependent fluorescence quenching by **Ru-2** with $\lambda_{max} = 499$ nm is fastest and most favorable for alkyne, followed by allene and then by alkene (alkyne **6** > allene **7** > alkene **5**), caused by the effect of the imidazolidine carbene ligand of **Ru-2** in the place of one phosphine (PCy_3) of **Ru-1** (Figure 3D and Table 1). Our results are in accord with the previous suggestion by Grubbs and coworkers that **Ru-1** and **Ru-2** possess different phosphine binding and dissociation behaviors that result in slower binding rate of alkene to **Ru-2** than **Ru-1**.[15] Our results also, for the first time, quantitatively show that catalysts **Ru-2**, **Mo-1** and **Mo-2** commonly favor alkyne over alkene or allene, and directly differentiate **Ru-2** from **Ru-1** by their completely different substrate preferences.

The Grubbs−Hoveyda catalysts (**Ru-3** and **Ru-4**) differ from the Grubbs analogues (**Ru-1** and **Ru-2**) in that the empty coordination site generated by the dissociation of a PCy_3 ligand is lightly protected by a weakly coordinating oxygen atom of an ether moiety. Considering the weak coordination nature of the oxygen atom, **Ru-3** and **Ru-4** should exhibit similar substrate preferences to their **Ru-1** and **Ru-2** analogues, respectively. Catalysts **Ru-3** and **Ru-4** exhibit small absorbance bands at 500 and 580 nm in CH_2Cl_2, respectively, which barely overlap with the fluorescence of the dye in the same solvent, not suitable for FRET study. Therefore we changed the reaction medium to *n*-hexane so that the fluorescence band of the substrates is shifted to 432 nm and overlaps with the huge absorbance bands of **Ru-3** and **Ru-4** at 363 and 377 nm, respectively (Figure 1C).

(15) Sanford, M. S.; Ulman, M.; Grubbs, R. H. *J. Am. Chem. Soc.* **2001**, *123*, 749.

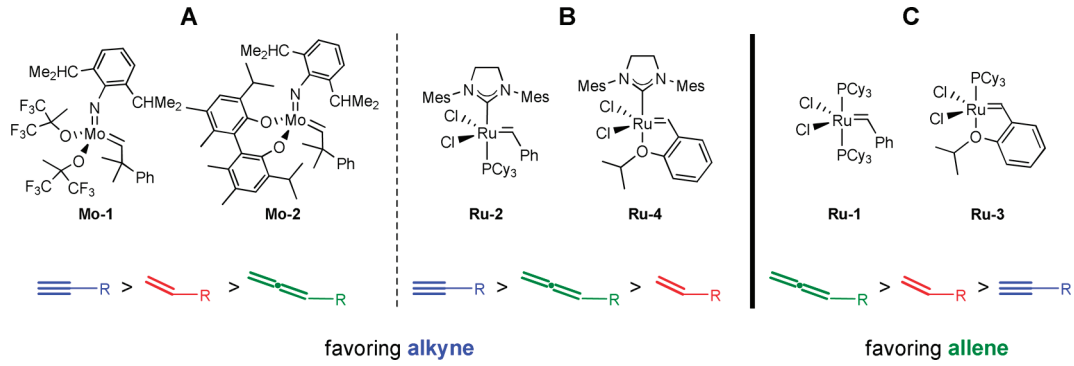

Figure 5. Summary of the substrate preferences of Mo and Ru catalysts studied. The substrate preferences are dependent on the molecular identity of the catalyst, exhibiting the preference order of (A) alkyne > alkene > allene for **Mo-1** and **Mo-2**, (B) allene > alkene > alkyne for **Ru-1** and **Ru-3**, and (C) alkyne > allene > alkene for **Ru-2** and **Ru-4**. Based on their favorite substrates, these catalysts can be categorized into two groups, namely, **Mo-1**, **Mo-2**, **Ru-2** and **Ru-4** favoring alkyne, and **Ru-1** and **Ru-3** favoring allene (A and B vs C).

As expected, catalyst **Ru-3** exhibits the same substrate association preference of allene **7** > alkene **5** > alkyne **6** as for **Ru-1**, and catalyst **Ru-4** demonstrates the substrate preference of alkyne **6** > allene **7** > alkene **5**, identical to that for **Ru-2** (Figure 3E,F and Table 1). In *n*-hexane, catalyst **Ru-1** with another absorbance at 330 nm also displayed the same substrate preference order as in CH_2Cl_2, confirming the general applicability of our FRET-based method (see Supporting Information). While some differences in the fluorescence quenching rate were observed, overall reactivity patterns remain the same.

Unlike the case of Mo-catalyzed olefin metathesis in which the rate determining step is the substrate association step, for the Ru case, low temperature NMR studies provided results supporting that the rate determining step is ancillary ligand decoordination for olefin metathesis,[16] and some quantum calculations support that the highest energy point is at a metallacyclobutene for enyne metathesis.[11] Thus, the obtained substrate-association preferences cannot be directly applied to answer previously unexplained Ru-catalyzed reaction patterns. On the other hand, it is rather surprising that some reaction patterns appear to be linked with the substrate association preferences although our experiment alone cannot justify the assumption that the initial substrate association determines the final outcome. For example, the observation that bisallene cross-metathesis reactions proceed well by **Ru-1**, but not by **Ru-2**,[6a] is in line with the relatively strong allene substrate preference of **Ru-1** compared with that of **Ru-2**. Additionally, much stronger alkyne preference of **Ru-2** than to alkene substrate can be in accordance with the result that only the alkyne group was transformed by **Ru-2** whereas the alkene group remains intact in the trimerization reaction of cyclooctenyne, an enyne cyclic compound with similarly distorted alkene and alkyne.[17] It should be noted, however, that although the substrate preferences appear to direct the reaction outcome, the current experimental data concerning only the initial substrate−catalyst association step alone cannot prove such dependence. To obtain the whole perspective, each plausible downstream process needs to be investigated, and in principle, this can be achieved by designing FRET pairs pertaining to such a step and using the same FRET-based method.[18]

In summary, our results demonstrate that the substrate preferences are dependent on the molecular identity of the catalyst, exhibiting the preference order of alkyne > alkene > allene for **Mo-1** and **Mo-2** presumably due to the similar electronic and molecular structure of the two catalysts, allene > alkene > alkyne for **Ru-1** and **Ru-3**, and alkyne > allene > alkene for **Ru-2** and **Ru-4**. Considering the weak coordination nature of the ether oxygen atom, **Ru-3** and **Ru-4** should exhibit similar substrate preferences to their **Ru-1** and **Ru-2** analogues, respectively. Based on their favorite substrates, these catalysts can be categorized into two groups, namely, **Mo-1**, **Mo-2**, **Ru-2** and **Ru-4** favoring alkyne, and **Ru-1** and **Ru-3** favoring allene (Figure 5). To fully understand the intricate play of energetics between substrates and catalysts, further theoretical studies on molecular orbital energy, as well as the investigation of the steric effect of the substrate, are necessary.

Conclusion

We quantitatively determined the catalyst−substrate relationships with association preferences of the representative Mo and Ru catalysts for metathesis reaction to their substrates, alkene, alkyne and allene using FRET-based method. The results provide new insight into the metathesis reactions along with answering the reaction initiation in enyne or allenyne metathesis and previously unexplained metathesis patterns. Due to our successful quantification of the Mo/Ru catalyst−substrate association interactions, diverse metal complex−substrate systems can now be quantitatively assessed and the newly found set of the catalyst−substrate association relationships might lead to new metal catalysis such as new tandem or multicomponent reaction methodologies, aided by much clarified reaction mechanisms.

Experimental Section

1. Synthesis of Compounds.

1.1. General. Common solvents were purified before use. Tetrahydrofuran (THF) and dichloromethane (CH_2Cl_2) were purified by distillation from sodium−benzophenone and calcium hydride respectively. Methanol and Et_3N (AldrichSeal) were used as received. All reagents were reagent grade and purified where necessary. "Water" refers to distilled water. Reactions were monitored by thin layer chromatography (TLC) using Whatman precoated silica gel plates. Flash column chromatography was performed over ultra pure silica gel (230−400 mesh) from Merck. ^{1}H NMR and ^{13}C NMR spectra were recorded on Varian 400-MR spectrometer and Bruker AVANCE 400 spectrometer using residual solvent peaks as an internal standard ($CHCl_3$, δ 7.24 ppm for proton and δ 77.0 ppm for carbon; acetone, δ 2.05 ppm for proton and δ

(16) van der Eide, E. F.; Piers, W. E. *Nat. Chem.* **2010**, *2*, 571.
(17) Carness, M.; Buccella, D.; Siegrist, T.; Steigerwald, M. L.; Nuckolls, C. *J. Am. Chem. Soc.* **2008**, *130*, 14078.
(18) Lim, S.-G.; Blum, S. A. *Organometallics* **2009**, *28*, 4643.

29.9 ppm for carbon; CH_3OH, δ 3.30 ppm for proton and δ 49.0 ppm for carbon). Multiplicities for ^{1}H NMR are designated as: s = singlet, d = doublet, dd = doublet of doublets, ddd = doublet of dd, dt = doublets of triplets, dq = doublet of quartets, td = triplet of doublets, t = triplet, q = quartet, m = multiplet, bs = broad singlet. Infrared spectra (IR) were recorded on a Bruker ALPHA-E FT-IR spectrometer and are reported in reciprocal centimeters (cm^{-1}). UV−visible spectra were recorded on Varian Cary 5000 spectrophotometer. High resolution mass spectra (HRMS) were obtained on Bruker microTOF-Q.

1.2. General Procedure for the Syntheses of Coumarin−Alkene 1, −Alkyne 2, −Allene 3, and −Alkane 4.

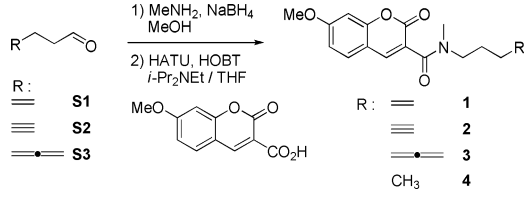

To a stirred solution of aldehyde (**S1**,[19] **S2**[20] or **S3**[21]) (110 mg, 1.34 mmol) in MeOH was added $MeNH_2$ (33 wt % in EtOH, 0.33 mL, 2.68 mmol), and the mixture was stirred at room temperature for 2 h. After the reaction mixture was cooled to 0 °C, $NaBH_4$ (25 mg, 0.67 mmol) was added and the resulting mixture was stirred at 0 °C for 30 min. After quenching with H_2O (3 mL) the mixture was extracted with CH_2Cl_2 (5 mL × 3), dried over $MgSO_4$, filtered, acidified with 2 M HCl in Et_2O (2 mL), and concentrated under reduced pressure. The solid crude product was washed with Et_2O to afford off-white solid. To a stirred solution of the solid (18.5 mg, 0.14 mmol), coumaric acid (15 mg, 0.068 mmol), HOBT (2 mg, 0.014 mmol), and HATU (52 mg, 0.14 mmol) in THF (0.22 mL) was added *i*-Pr_2NEt (0.060 mL, 0.34 mmol), and the mixture was stirred overnight at room temperature in a dark atmosphere. Saturated NH_4Cl (1 mL) was added, and the resulting mixture was extracted with CH_2Cl_2 (1 mL × 3). The combined organic layers were dried over $MgSO_4$, filtered, and concentrated under reduced pressure. The crude product was purified by prep. TLC (EtOAc: *n*-hexane = 6:4) to give coumarin-conjugated compound as yellowish film-like solid.

1.3. Coumarin−Alkene 1 (51%). TLC (*n*-hexane:EtOAc, 40: 60 v/v): R_f = 0.31. ^{1}H NMR (400 MHz, CD_3OD): δ 7.83 (s, 0.5H), 7.76 (s, 0.5H), 7.39 (d, J = 8.7 Hz, 1H), 6.85 (dt, J = 8.6 Hz, 2.3 Hz, 1H), 6.80 (d, J = 1.9 Hz, 1H), 5.82 (m, 0.5H), 5.64 (m, 0.5H), 5.05 (d, J = 17.1 Hz, 0.5H), 4.97 (d, J = 10.3 Hz, 0.5H), 4.92 (d, J = 17.1 Hz, 0.5H), 4.86 (d, J = 10.2 Hz, 0.5H), 3.86 (s, 3H), 3.50 (t, J = 7.4 Hz, 1H), 3.24 (t, J = 7.5 Hz, 1H), 3.04 (s, 1.5H), 2.95 (s, 1.5H), 2.12 (q, J = 7.0 Hz, 1H), 1.94 (q, J = 6.9 Hz, 1H), 1.69 (m, 2H). ^{13}C NMR (100 MHz, CD_3OD): δ 165.4, 165.3, 163.6, 158.4, 158.0, 156.1, 156.0, 143.2, 142.7, 137.8, 137.1, 129.5, 129.4, 122.3, 122.0, 115.5, 115.1, 113.2, 112.0, 111.9, 100.64, 100.60, 55.9, 50.4, 47.3, 36.3, 32.7, 30.8, 30.4, 27.1, 26.1. IR (film) cm^{-1}: 3424, 2924, 2853, 1717, 1607, 1563, 1507, 1441, 1403, 1367, 1291, 1241, 1196, 1157, 1137, 1117, 1024, 912, 833, 620. UV/vis: λ_{max} 345 nm. Fluorescence: λ_{max} 412 nm (toluene). HRMS (*m*/*z*): $[M + Na]^+$ calcd for $C_{17}H_{19}NNaO_4$, 324.1212; found, 324.1206.

1.4. Coumarin−Alkyne 2 (62%). TLC (*n*-hexane:EtOAc, 40: 60 v/v): R_f = 0.31. ^{1}H NMR (400 MHz, CD_3OD): δ 7.84 (s, 0.5H), 7.78 (s, 0.5H), 7.39 (d, J = 8.6 Hz, 1H), 6.85 (dt, J = 8.6 Hz, 2.1 Hz, 1H), 6.80 (t, J = 2.7 Hz, 1H), 3.86 (s, 3H), 3.60 (t, J = 7.1 Hz, 1H), 3.40 (t, J = 7.1 Hz, 1H), 3.05 (s, 1.5H), 2.99 (s, 1.5H), 2.30 (td, J = 7.1 Hz, 2.6 Hz, 1H), 2.12 (td, J = 6.6 Hz, 2.6 Hz, 1H), 1.96 (t, J = 2.6 Hz, 0.5H), 1.88 (m, 1H), 1.78 (m, 1H), 1.67 (t, J = 2.6 Hz, 0.5H). ^{13}C NMR (100 MHz, CD_3OD): δ 165.6, 165.5, 163.7, 163.5, 158.5, 158.0, 156.2, 156.0, 143.3, 142.9, 129.51, 129.46, 122.1, 121.9, 113.3, 113.2, 111.99, 111.96, 100.61, 100.59, 83.6, 82.7, 69.3, 68.8, 55.9, 49.6, 46.9, 38.6, 36.7, 32.7, 26.6, 25.8, 15.9, 15.5. IR (film) cm^{-1}: 3435, 3284, 2935, 2848, 1717, 1611, 1565, 1508, 1441, 1404, 1369, 1292, 1243, 1196, 1027, 836, 637, 525. UV/vis: λ_{max} 345 nm. Fluorescence: λ_{max} 412 nm (toluene). HRMS (*m*/*z*): $[M + Na]^+$ calcd for $C_{17}H_{17}NNaO_4$, 322.1055; found, 322.1061.

1.5. Coumarin−Allene 3 (56%). TLC (*n*-hexane:EtOAc, 40: 60 v/v): R_f = 0.30. ^{1}H NMR (400 MHz, CD_3OD): δ 7.83 (s, 0.5H), 7.76 (s, 0.5H), 7.39(d, J = 8.6 Hz, 1H), 6.87 (dt, J = 8.6 Hz, 2.1 Hz, 1H), 6.81 (d, J = 2.3 Hz, 1H), 5.14 (m, 0.5H), 4.97 (m, 0.5H), 4.68 (m, 1H), 4.52 (m, 1H), 3.86 (s, 3H), 3.53 (t, J = 7.3 Hz, 1H), 3.28 (t, J = 7.4 Hz, 1H), 3.05 (s, 1.5H), 2.96 (s, 1.5H), 2.09 (m, 1H), 1.88 (m, 1H), 1.70 (m, 2H). ^{13}C NMR (100 MHz, CD_3OD): δ 208.5, 208.3, 165.4, 165.3, 163.6, 163.6, 158.4, 158.0, 156.1, 156.0, 143.1, 142.6, 129.5, 129.4, 122.3, 122.1, 113.2, 112.0, 111.9, 100.64, 100.61, 89.3, 88.8, 75.6, 75.3, 55.9, 50.3, 47.2, 36.4, 32.8, 27.0, 26.1, 25.2, 24.7. IR (film) cm^{-1}: 3419, 2923, 2852, 1953, 1714, 1606, 1562, 1506, 1440, 1402, 1367, 1290, 1241, 1192, 1147, 1116, 1021, 798, 611, 520. UV/vis: λ_{max} 345 nm. Fluorescence: λ_{max} 412 nm (toluene). HRMS (*m*/*z*): $[M + Na]^+$ calcd for $C_{18}H_{19}NNaO_4$, 336.1212; found, 336.1216.

1.6. Coumarin−Alkane 4. 4 was synthesiszed from commercially available *N*-methylbutylamine (88%). TLC (*n*-hexane: EtOAc, 40:60 v/v): R_f = 0.32. ^{1}H NMR (400 MHz, CD_3OD): δ 7.82 (s, 0.5H), 7.76 (s, 0.5H), 7.39 (d, J = 8.6 Hz, 1H), 6.84 (dt, J = 8.6 Hz, 2.1 Hz, 1H), 6.80 (d, J = 2.3 Hz, 1H), 3.86 (s, 3H), 3.49 (t, J = 7.4 Hz, 1H), 3.23 (t, J = 7.5 Hz, 1H), 3.04 (s, 1.5H), 2.95 (s, 1.5H), 1.61 (m, 1H), 1.56 (m, 1H), 1.40 (m, 1H), 1.20 (m, 1H), 0.94 (t, J = 7.3 Hz, 1.5H), 0.82 (t, J = 7.3 Hz, 1.5H). ^{13}C NMR (100 MHz, CD_3OD): δ 165.2, 163.6, 158.0, 156.1, 143.0, 142.5, 129.5, 129.4, 122.4, 122.2, 113.2, 112.0, 111.9, 100.7, 100.6, 55.9, 50.9, 47.5, 36.3, 32.7, 30.2, 29.0, 20.0, 19.7, 13.9, 13.7. IR (film) cm^{-1}: 3384, 2957, 2923, 2853, 1719, 1608, 1563, 1457, 1403, 1367, 1242, 1218, 1158, 1115, 1023, 801, 519. UV/vis: λ_{max} 345 nm. Fluorescence: λ_{max} 412 nm (toluene). HRMS (*m*/*z*): $[M + Na]^+$ calcd for $C_{16}H_{20}NNaO_4$, 312.1212; found, 312.1213.

1.7. Synthesis of Dapoxyl−Allene 7.

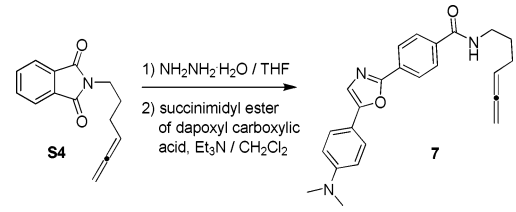

A mixture of **S4**[22] (500 mg, 2.20 mmol) and $H_2NNH_2 \cdot H_2O$ (80% in H_2O, 0.7 mL) in THF (3 mL) was stirred overnight at 40 °C and for 5 h at room temperature. The reaction mixture was filtered and rinsed with Et_2O (20 mL). The filtrate was washed with 1 N NaOH (4 mL) and brine (4 mL), dried over $MgSO_4$, filtered, acidified with 2 M HCl in Et_2O (3 mL), and concentrated under reduced pressure. The solid crude product was washed with EtOAc and CH_2Cl_2 to give hexa-4,5-dien-1-aminium chloride[23] as colorless solid (168 mg, 57%): ^{1}H NMR (400 MHz, CD_3OD) δ 5.18 (m, 1H), 4.73 (m, 2H), 2.96 (t, J = 7.6 Hz, 2H), 2.09 (m, 2H), 1.77 (m, 2H); ^{13}C NMR (100 MHz, CD_3OD) δ 208.7, 88.0, 74.6, 39.0, 26.6, 24.7. To a mixture of the hexa-4,5-dien-1-aminium chloride (1.2 mg, 9.05 μmol) and activated dapoxyl (2.5 mg, 6.17 μmol) in CH_2Cl_2

(19) Kelly, B. D.; Allen, J. M.; Tundel, R. E.; Lambert, T. H. *Org. Lett.* **2009**, *11*, 1381.
(20) Adams, T. C.; Dupont, A. C.; Carter, J. P.; Kachur, J. F.; Guzewska, M. E.; Rzeszotarski, W. J.; Farmer, S. G.; Noronha-Blob, L.; Kaiser, C. *J. Med. Chem.* **1991**, *34*, 1585.
(21) Tsukamoto, H.; Matsumoto, T.; Kondo, Y. *J. Am. Chem. Soc.* **2008**, *130*, 388.
(22) Trost, B. M.; Pinkerton, A. B.; Seidel, M. *J. Am. Chem. Soc.* **2001**, *123*, 12466.
(23) Jonasson, C.; Horváth, A.; Bäckvall, J.-E. *J. Am. Chem. Soc.* **2000**, *122*, 9600.

(0.2 mL) was added Et_3N (3.8 μL, 27.3 μmol), and the resulting mixture was stirred for 20 min at 0 °C. The mixture was diluted with EtOAc (3 mL), washed with saturated NH_4Cl (0.5 mL) and brine (0.5 mL), dried over $MgSO_4$, filtered, and concentrated under reduced pressure. The crude product was purified by preparative TLC to give dapoxyl−allene **7** (2.3 mg, 95%) as a pale green solid. TLC (*n*-hexane:EtOAc, 30:70 v/v): $R_f = 0.18$. ^{1}H NMR (400 MHz, acetone-d_6): δ 8.15 (d, $J = 8.4$ Hz, 2H), 8.02 (d, $J = 8.4$ Hz, 2H), 7.87 (bs, 1H), 7.68 (d, $J = 8.8$ Hz, 2H), 7.45 (s, 1H), 6.84 (d, $J = 8.8$ Hz, 2H), 5.20 (m, 1H), 4.69 (m, 2H), 3.47 (q, $J = 6.0$ Hz, 2H), 3.02 (s, 6H), 2.12 (m, 2H), 1.76 (m, 2H);. ^{13}C NMR (100 MHz, acetone-d_6): δ 209.5, 206.1, 166.6, 159.7, 153.8, 151.8, 137.1, 130.9, 128.7, 126.6, 126.4, 122.0, 116.6, 113.2, 90.2, 75.3, 40.4, 40.1, 26.5. IR (film) cm^{-1}: 3329, 2924, 2854, 2360, 2341, 1956, 1728, 1638, 1611, 1509, 1364, 1288, 1125, 853, 815, 714. UV/vis: λ_{max} 366 nm. Fluorescence: λ_{max} 566 nm (MeOH), 548 nm (EtOH), 545 nm (CH_3CN), 530 nm (*i*-PrOH), 521 nm (acetone), 508 nm (CH_2Cl_2), 488 nm (EtOAc), 454 nm (*m*-xylene), 432 nm (*n*-hexane). HRMS (*m*/*z*): $[M + H]^+$ calcd for $C_{24}H_{26}N_3O_2$, 388.2025; found, 388.2024.

2. Measurement of Time-Dependent Fluorescence Quenching Signal.

2.1. Home-Built Spectrometer. Time-dependent fluorescence quenching signal was measured by a home-built spectrofluorometer that consists of a Nd:YAG nanosecond laser, a grating and a CCD detector. The third harmonic (355 nm) of an Nd:YAG laser (Brilliant B) was used as the excitation beam. Laser pulses with 10 μJ were focused to about 5 mm diameter. Sample solution in 10 by 10 mm quartz cuvette was put in a temperature-controlled holder. Fluorescence light was gathered by two lenses located at 90° from the laser path and spatially resolved by wavelength with the grating. Resolved fluorescence spectrum was recorded from 350 to 650 nm by a gated CCD detector. The measurement speed was 10 Hz, and typically 150 or 300 (corresponding to 15 or 30 s) spectra were averaged to get a time-dependent spectrum at a certain time point.

2.2. Measurement of Fluorescence Quenching Signal. The time-dependent fluorescence quenching signal was measured by a home-built spectrofluorometer consisting of a Nd:YAG nanosecond laser, a grating and a CCD detector (for more details, see Supporting Information). During the fluorescence measurement, all the samples were treated with anhydrous solvents under Ar. A 3 mL solution of a substrate in toluene (for **Mo-1** and **Mo-2**), CH_2Cl_2 (for **Ru-1** and **Ru-2**) or *n*-hexane (for **Ru-3** and **Ru-4**) in a quartz cuvette with Ar balloon was put in a temperature-controlled holder. The sample was excited at 355 nm, and the fluorescence spectrum was recorded from 320 to 600 nm for toluene solutions, 350 to 650 nm for CH_2Cl_2 solutions, and 360 to 560 nm for *n*-hexane solutions. Before a catalyst was added, a spectrum was acquired to provide a reference spectrum at time zero. 1 or 2 equiv of the catalyst (0.3 mM CH_2Cl_2 solution) was added to the substrate solution using a 25 μL syringe, and the fluorescence spectrum was obtained as a function of time.

Acknowledgment. We thank Hee-Yoon Lee (KAIST), Tae-Lim Choi (SNU) and JeanSun Lim for helpful discussions on metathesis reaction or experimental assistance. This work was partially supported by Creative Research Initiatives (Center for Time-Resolved Diffraction) of MEST/NRF and the NRF grant (No.2010-0001953) funded by MEST. We acknowledge the support from the WCU program.

Supporting Information Available: All time-dependent quenching traces and their conditions, substrate absorbance change during fluorescence quenching, time-dependent fluorescence quenching of the substrates by **Ru-1** in *n*-hexane, global fitting analysis of FRET data, and ^{1}H and ^{13}C NMR spectra of substrates **1**−**4** and **7**. This material is available free of charge via the Internet at http://pubs.acs.org.

JA104193S